UCRL-11982

University of California

Ernest O. Lawrence Radiation Laboratory

TWO-WEEK LOAN COPY

This is a Library Circulating Copy which may be borrowed for two weeks. For a personal retention copy, call Tech. Info. Division, Ext. 5545

THE REACTION $K^- p \rightarrow \Lambda\omega$: 1.2 TO 1.8 BeV/c

Berkeley, California

DISCLAIMER

This document was prepared as an account of work sponsored by the United States Government. While this document is believed to contain correct information, neither the United States Government nor any agency thereof, nor the Regents of the University of California, nor any of their employees, makes any warranty, express or implied, or assumes any legal responsibility for the accuracy, completeness, or usefulness of any information, apparatus, product, or process disclosed, or represents that its use would not infringe privately owned rights. Reference herein to any specific commercial product, process, or service by its trade name, trademark, manufacturer, or otherwise, does not necessarily constitute or imply its endorsement, recommendation, or favoring by the United States Government or any agency thereof, or the Regents of the University of California. The views and opinions of authors expressed herein do not necessarily state or reflect those of the United States Government or any agency thereof or the Regents of the University of California.

Presented by M. L. Stevenson at
the 1965 Boulder Conference on
Particle Physics, Boulder, Colorado,
August 9-20, 1965 and submitted
to Physical Review

UCRL-11982

UNIVERSITY OF CALIFORNIA
Lawrence Radiation Laboratory
Berkeley, California

AEC Contract No. W-7405-eng-48

THE REACTION $K^-p \rightarrow \Lambda\omega$: 1.2 TO 1.8 BeV/c

Philippe Eberhard, Stanley M. Flatté, Darrell O. Huwe,
Janice Button-Shafer, Frank T. Solmitz, and M. Lynn Stevenson

October 13, 1965

THE REACTION $K^-p \rightarrow \Lambda\omega$: 1.2 TO 1.8 BeV/c *

Philippe Eberhard, Stanley M. Flatté,† Darrell O. Huwe,
Janice Button-Shafer, Frank T. Solmitz, and M. Lynn Stevenson

Lawrence Radiation Laboratory
University of California
Berkeley, California

October 13, 1965

ABSTRACT

Both total and differential cross sections for the reaction $K^-p \rightarrow \Lambda\omega$ have been determined within the following region of s, the total c.m. energy squared, and t, the four-momentum-transfer squared: $(1.88\ \text{BeV})^2 < s < (2.09\ \text{BeV})^2$ and $-(1.28\ \text{BeV})^2 < t < -(0.29\ \text{BeV})^2$. The decay angular correlations of the Λ decay products $(p\pi^-)$ and the ω decay products $(\pi^+\pi^-\pi^0)$ have been systematically determined. In three subregions of s and t, the six production amplitudes that describe the reaction have been determined. It is shown that no simple exchange models explain the data and that no striking resonance formation in the direct channel is taking place.

THE REACTION $K^-p \rightarrow \Lambda\omega$: 1.2 TO 1.8 BeV/c

Philippe Eberhard, Stanley M. Flatté, Darrell O. Huwe,
Janice Button-Shafer, Frank T. Solmitz, and M. Lynn Stevenson

Lawrence Radiation Laboratory
University of California
Berkeley, California

October 13, 1965

I. INTRODUCTION

We report here on one of the several two-body final states that are produced in K^-p interactions in the interval of incident momentum, 1.2 to 1.8 BeV/c. The initial state, an isospin mixture of T = 0 and T = 1, can energetically produce systems in the center-of-mass (c. m.) frame, with total mass squared s between $(1.88\ \text{BeV})^2$ and $(2.09\ \text{BeV})^2$. We refer to this as the s-channel. The reaction

$$K^-p \rightarrow \Lambda\omega \tag{1s}$$

has been observed in the 72-inch hydrogen bubble chamber. In this article we deal only with events in which the decay of the Λ into $p\pi^-$ and the decay of the ω into $\pi^+\pi^-\pi^0$ have resulted in a V + two-prong event. The identification method for the reaction

$$K^-p \rightarrow \Lambda\,\pi^+\pi^-\pi^0 \tag{2}$$

was given in detail in the previous paper.[1]

In Table I we have expressed the amount of data at each momentum in terms of the number of events per millibarn of cross section. Figure 1(a) shows the three-pion mass spectrum for all the data; in Sec. VI we describe how we decide the number of ω events present and how we determine the behavior of the ω events by subtracting background.

Because reaction (1s) has a pure T = 0 final state, it might disclose the existence of T = 0, Y = 0 resonant states in the mass interval corresponding

to the interval of total energy in the center of mass. The symbol Y represnets the hypercharge, and is the sum of the baryon number and strangeness quantum number. Regge recurrences of $Y^0(1405)$ and $Y^0(1525)$ might be expected here. [See Fig. 4(a).]

Because the total cross section as a function of energy shows no obvious peak, no strong resonance formation is indicated. (See Fig. 2.) The absence of rapid changes in the production-angle distribution as a function of energy is further indication that a resonance is not dominating. (See Fig. 3.) The distributions in t at each energy-squared s correspond to distributions in production angle.

There are two important associated channels from which the four particles which take part in reaction (1s) (or their antiparticles) may be contemplated. In one of these channels our experiment appears as the process

$$\bar{\Lambda}p \rightarrow K^+\omega \qquad (1t)$$

with total mass squared t between $-(1.28\ \text{BeV})^2$ and $-(0.29\ \text{BeV})^2$. Intermediate states in this, the t-channel, have quantum numbers $T = 1/2$, $T_z = +1/2$, and $Y = 1$. The nearest known physical states with these quantum numbers are K^+ at $t = (0.495\ \text{BeV})^2$ and K^{*+} at $t = (0.891\ \text{BeV})^2$. [See Fig. 4(b).]

In the other channel, our experiment appears as the process

$$\omega p \rightarrow K^+\Lambda \qquad (1u)$$

with the total mass squared u between $-(1.25\ \text{BeV})^2$ and $-(0.34\ \text{BeV})^2$. The least-massive intermediate state--with quantum numbers $T = 1/2$, $T_z = +1/2$, and $Y = 1$--in this, the u channel, is the proton at $u = (0.938\ \text{BeV})^2$. [See Fig. 4(c).]

For our experiment, reactions (1t) and (1u) obviously occur in the unphysical region. The presence of (a) K^+ and K^{*+} states in the t-channel, (b) the proton state in the u-channel, and (c) other simple systems with the correct quantum numbers for these channels, is expected to influence, by the mechanism of the exchange model, what we observe in the physical region of the s-channel. In Sec. XII we present evidence that no simple exchanges in either the t or the u channel dominate reaction (1s). The combination of many exchanges in various channels may provide a satisfactory fit to the data; however, we feel this would indicate only the flexibility of a large number of parameters.

According to SU(3) symmetry, reaction (1s) is the interaction of a member of the pseudoscalar octet with a member of the baryon octet to produce another member of that baryon octet and a vector meson that is presumed to be a linear combination of ω_8, a member of an octet of vector mesons, and ω_1, an SU(3) singlet. Some of the decay modes of the ω discussed in the previous paper[1] bear upon this latter presumption, called ϕ-ω mixing.

We find that the reaction is not explained by the simple models available. We have, therefore, attempted to exhibit our data in an easily understood manner, convenient for the testing of any future theory.

II. DEFINITION OF INTERNAL VARIABLES

Let us define the internal variables of the reaction. We limit our consideration to those events in which the ω decays into $\pi^+\pi^-\pi^0$ and the Λ decays into $p\pi^-$.

With the four momenta and masses labeled as in Fig. 5, we define s, t, and u by

$$s = (P_1 + q_1)^2$$
$$t = (q_2 - q_1)^2$$
$$u = (P_2 - q_1)^2.$$

Conservation of energy-momentum implies that

$$s + t + u = \mu_1^2 + \mu_2^2 + M_1^2 + M_2^2;$$

hence only two of the three variables (s, t, and u) are independent.

Unit vectors that we define in the ω rest frame are

$\underset{\sim}{n}$ = normal to the plane of the pions from the ω decay ($\underset{\sim}{\pi}^- \times \underset{\sim}{\pi}^+$)

$\underset{\sim}{N}$ = normal to the production plane $\underset{\sim}{K} \times \underset{\sim}{\omega}$ (defined in the center-of-mass frame and unchanged when shifted to the ω rest frame.)

$\underset{\sim}{X}$, $\underset{\sim}{Y}$, $\underset{\sim}{N}$ = an orthogonal set of axes defined by the production process (e.g., $\underset{\sim}{P}_1$, $\underset{\sim}{N} \times \underset{\sim}{P}_1$, $\underset{\sim}{N}$).

Unit vectors that we define in the Λ rest frame are

$\underset{\sim}{\pi}$ = direction of the pion from the Λ decay

$\underset{\sim}{N}$ = normal to the production plane (same as in ω rest frame)

$\underset{\sim}{X}'$, $\underset{\sim}{Y}'$, $\underset{\sim}{N}'$ = an orthogonal set of axes defined by the production process (e.g., $\underset{\sim}{q}_1$, $\underset{\sim}{N} \times \underset{\sim}{q}_1$, $\underset{\sim}{N}$).

III. EXPRESSIONS FOR CROSS SECTIONS

Byers and Yang[2] and Berman and Oakes[3] have exhibited the general dependence of this reaction on the angles formed in the decays of the final-state particles, given an unpolarized target. Huff[4] has also discussed this reaction. Ademollo and Gatto[5] treated the production characteristics of reactions of this type by means of a density-matrix formalism; such a treatment is the connecting link between the correlations in Sec. III and the production amplitudes in Sec. IX. Of course, the spins and parities of the ω and Λ are taken to be 1^- and $1/2^+$, respectively. We may express the entire dependence of the cross section on internal variables as follows:

$$d^5\sigma = \Big\{ F_1(\underset{\sim}{n}\cdot\underset{\sim}{N})^2 + F_2(\underset{\sim}{n}\cdot\underset{\sim}{X})^2 + F_3(\underset{\sim}{n}\cdot\underset{\sim}{Y})^2 + F_4(\underset{\sim}{n}\cdot\underset{\sim}{X})(\underset{\sim}{n}\cdot\underset{\sim}{Y}) + F_5(\underset{\sim}{n}\cdot\underset{\sim}{N})^2(\underset{\sim}{\pi}\cdot\underset{\sim}{N})$$

$$+ F_6(\underset{\sim}{n}\cdot\underset{\sim}{X})^2(\underset{\sim}{\pi}\cdot\underset{\sim}{N}) + F_7(\underset{\sim}{n}\cdot\underset{\sim}{Y})^2(\underset{\sim}{\pi}\cdot\underset{\sim}{N}) + F_8(\underset{\sim}{n}\cdot\underset{\sim}{X})(\underset{\sim}{n}\cdot\underset{\sim}{Y})(\underset{\sim}{\pi}\cdot\underset{\sim}{N}) + F_9(\underset{\sim}{n}\cdot\underset{\sim}{N})(\underset{\sim}{n}\cdot\underset{\sim}{X})(\underset{\sim}{n}\cdot\underset{\sim}{X}')$$

$$+ F_{10}(\underset{\sim}{n}\cdot\underset{\sim}{N})(\underset{\sim}{n}\cdot\underset{\sim}{Y})(\underset{\sim}{n}\cdot\underset{\sim}{X}') + F_{11}(\underset{\sim}{n}\cdot\underset{\sim}{N})(\underset{\sim}{n}\cdot\underset{\sim}{X})(\underset{\sim}{n}\cdot\underset{\sim}{Y}') + F_{12}(\underset{\sim}{n}\cdot\underset{\sim}{N})(\underset{\sim}{n}\cdot\underset{\sim}{Y})(\underset{\sim}{n}\cdot\underset{\sim}{Y}') \Big\}$$

$$\cdot \left\{ \frac{3}{(4\pi)^2} \, d\Omega_{\underset{\sim}{\pi}} \, d\Omega_{\underset{\sim}{n}} \, dt \right\} .$$

Each F_i is an unknown function of s and t, and depends on the dynamics of the process.

It is convenient to introduce another parameterization of the cross-section formula:

$$d^5\sigma = C(s,t) \Big\{ f_1(\underset{\sim}{n}\cdot\underset{\sim}{N})^2 + f_2(\underset{\sim}{n}\cdot\underset{\sim}{X})^2 + f_3(\underset{\sim}{n}\cdot\underset{\sim}{Y})^2 + f_4(\underset{\sim}{n}\cdot\underset{\sim}{X})(\underset{\sim}{n}\cdot\underset{\sim}{Y})$$

$$+ f_5(\underset{\sim}{n}\cdot\underset{\sim}{N})^2(\underset{\sim}{\pi}\cdot\underset{\sim}{N}) + \ldots \Big\} \left\{ \frac{3}{(4\pi)^2} \, d\Omega_{\underset{\sim}{\pi}} \, d\Omega_{\underset{\sim}{n}} \, dt \right\}$$

with the subsidiary condition $f_1 + f_2 + f_3 = 1$, which is the normalization condition after integration over the two solid angles involved.

By this parameterization we have provided a convenient normalization for the dependence of the cross section on the decay angles of the Λ and ω. That is, the dependence of the cross section on the decay angles (which means the dependence on the spin alignments of the Λ and ω) is contained in the $\{f_i\}$ in the form of a probability density whose integral is 1. Thus

$$d\sigma = \iint d^5\sigma \; d\Omega_{\underset{\sim}{\pi}} \; d\Omega_{\underset{\sim}{n}} = C(s,t)dt \iint \left\{ f_1 (n \cdot N)^2 + \ldots \right\} \frac{3}{(4\pi)^2} \; d\Omega_{\underset{\sim}{\pi}} \, d\Omega_{\underset{\sim}{n}}$$

$$d\sigma = C(s,t)dt$$

$$C(s,t) = \frac{d\sigma}{dt} \quad .$$

Thus $C(s,t)$ is the differential cross section, integrated over all decay angles, of the reaction taking place as a given s and t.

The total cross section is given by $\sigma_T(s) = \int C(s,t)dt$.

IV. GENERAL MODEL

At this point we might tabulate $d\sigma/dt$ and the set of f_i as a function of s and t. However, we still face the problem of choosing the vectors $\underset{\sim}{X}'$, $\underset{\sim}{Y}'$ and $\underset{\sim}{X}$, $\underset{\sim}{Y}$ in the Λ and the ω rest frames, respectively. If we could do our experiment at a unique s and a unique t, then, in each frame, any choice would be related to any other by a simple rotation around the normal. However, since we must average over rather large regions of s and t, it behooves us to choose our axes carefully. The choice is determined by the characteristics of the model being tested.

Most current theories have as a basis the idea of exchanged particles, as expressed, for example, in Feynman diagrams or unitarity graphs. Figures 4(a), 4(b), and 4(c) represent exchanges of the least-massive particles allowed in the three possible channels in $Kp \rightarrow \Lambda\omega$ -- the s, t, and u channels. With this model the correct choice of axes is apparent. In the u channel the appropriate axes in the ω rest frame are $\underset{\sim}{P}_1$, $\underset{\sim}{N} \times \underset{\sim}{P}_1$, $\underset{\sim}{N}$, and in the Λ rest frame they are $\underset{\sim}{q}_1$, $\underset{\sim}{N} \times \underset{\sim}{q}_1$, $\underset{\sim}{N}$. In the t channel the two sets are $\underset{\sim}{q}_1$, $\underset{\sim}{N} \times \underset{\sim}{q}_1$, $\underset{\sim}{N}$, and $\underset{\sim}{P}_1$, $\underset{\sim}{N} \times \underset{\sim}{P}_1$, $\underset{\sim}{N}$. In the s channel we have $\underset{\sim}{P}_2$, $\underset{\sim}{N} \times \underset{\sim}{P}_2$, $\underset{\sim}{N}$ and $\underset{\sim}{q}_2$, $\underset{\sim}{N} \times \underset{\sim}{q}_2$, $\underset{\sim}{N}$. At this point then we are concerned with tabulating our data in three different ways:
(a) the t-channel set, which includes values of $d\sigma/dt$ and $\{f_i\}$ at various values of s and t, and where $\{f_i\}$ are determined with the sets of axes associated with the t channel; (b) the u-channel set, which includes values of $d\sigma/du$ and $\{f_i\}$ at various values of s and u, and where $\{f_i\}$ are determined with the axes appropriate to the u channel; and (c) the s-channel set, which includes values of σ_T and $\{f_i\}$ at various values of s, and where $\{f_i\}$ are determined with the axes appropriate to the s channel.

V. EXPERIMENTAL CALCULATIONS

The quantities $d\sigma/dt$, $d\sigma/du$, and σ_T were obtained by a simple counting of events in a given region of s and t, or s and u, or s. Knowledge of the over-all cross sections (see Sec. XI) was then used to provide differential cross sections. The only problem here is background subtraction, which is discussed in the next section.

The maximum-likelihood technique was used to determine $\{f_i\}$. For each event we have a probability density that is a function of the twelve f_i

$$P_k = f_1(\underset{\sim}{n}\cdot \underset{\sim}{N})_k^2 + f_2(\underset{\sim}{n}\cdot \underset{\sim}{X})_k^2 + f_3(\underset{\sim}{n}\cdot \underset{\sim}{Y})_k^2 + \cdots$$

where the vectors have been evaluated for the particular event, as the subscript k indicates.

For a sample of N events, the likelihood $\mathcal{L}$ is,

$$\mathcal{L} = \prod_{k=1}^{N} P_k .$$

We maximize $\mathcal{L}$ by maximizing the logarithm of $\mathcal{L}$. We vary only eleven of the parameters $\{f_i\}$ since there is one constraint. The logarithm of $\mathcal{L}$ is

$$\ln\mathcal{L} = \sum_{k=1}^{N} \ln P_k .$$

Only one extremum can exist for our likelihood, and it is a maximum. Both of these facts are a consequence of the linearity of P_k as a function of the parameters $\{f_i\}$.

VI. BACKGROUND

If we look at the three-pion mass spectra in the reaction $Kp \rightarrow \Lambda\, \pi^+\pi^-\pi^0$, we see a prominent ω peak. (See Fig. 1.) Under this peak we also see a significant background, which we judged from the regions adjacent to the peak. By sketching a curve through the regions next to the ω peak, we estimate the number of non-ω events in the region of the three-pion mass between 750 and 815 MeV. We assume that the remainder in this region are events of the reaction $Kp \rightarrow \Lambda\omega$.

Let us call the 750 to 815-MeV region the ω region, and the two regions 685 to 750 MeV and 815 to 880 MeV, combined, the control region. Let N_B be the number of background events in the ω region, and N_C the number of events in the control region. We are dealing with a spectrum at a given s. To find the number of ω events N_ω in a certain region of t, we use $N_\omega = N - (N_B/N_C)\,(M)$, where N is the number of events in the ω region and in the region of t under discussion, and M is the number of events in the control region and in the region of t under discussion. Of course, if the region of t is large enough, we can do an independent background subtraction.

Treating background in determinations of $\{f_i\}$ is only slightly more complicated. The $\{f_i\}_\omega$ for events in the ω region is determined with the technique described in Sec. III, and another set, $\{f_i\}_c$ is determined for the events in the control region. Both sets are normalized to a total integral of one, so that the expression for the $\{f_i\}$ for the ω events is

$$f_i = \frac{1}{N_\omega} \left\{ N\, f_{i\omega} - (N_B/N_C)(M)\, f_{ic} \right\} .$$

VII. TABULATION OF ANGULAR CORRELATIONS AND OTHER DATA

A. The t-Channel Set (Table II)

Figure 6(a) shows the regions of s and t where the data have been combined. For the t-channel set, it is convenient to tabulate the following quantities:

s_{min} and s_{max}	the limits on the interval of s $(BeV)^2$
t_{min} and t_{max}	the limits on the interval of t $(BeV)^2$
$\sigma(s)$	the average cross section over the interval in s (mb)
N(s)	the number of events in the interval of s (regardless of t) in the ω region
N(s, t)	the number of events in the interval of s and the interval of t and in the ω region
BG(s, t)	the number of background events in the intervals of s and t and in the ω region
$d\sigma/dt$	the average differential cross section over the intervals of s and t for the reaction $Kp \rightarrow \Lambda\omega \rightarrow \Lambda\pi^+\pi^-\pi^0$ (mb/BeV^2)

B. The u-Channel Set (Table III)

Figure 6(b) presents the regions of s and u where the data have been combined. Quantities for the u-channel set are completely analogous to those for the t-channel set.

C. The s-Channel Set (Table IV)

We have tabulated s_{min} and s_{max}, N(s), $\sigma(s)$, and BG(s) (the number of background events in the s interval and the ω region).

We have not separated the s-channel data into regions of t because the presence of a resonance (s-channel exchange) should affect the

dependence on s most strongly. We have used small intervals of s, therefore, and we then do not have enough data to separate further into regions of t.

VIII. ERRORS

The errors on cross sections are treated in the usual manner for counting experiments. The errors on the f_i are more complex.

The maximum-likelihood routine we used yields an error matrix (obtained from inverting the second-derivative matrix) for the eleven f_i that were varied in the search. Thus we have all the correlated errors, and since the twelfth parameter is a function of the other eleven ($f_1 = 1 - f_2 - f_3$), we may find its error correlations also. When we list the error for an f_i, we are listing the square root of the diagonal element of the error matrix corresponding to that f_i. Thus the error matrix is

$$\left\langle \delta f_i \, \delta f_j \right\rangle = \frac{1}{(N_\omega)^2} \left\{ N^2 \left\langle \delta f_{i\omega} \, \delta f_{j\omega} \right\rangle - \left(\frac{N_B M}{N_C} \right)^2 \left\langle \delta f_{ic} \, \delta f_{jc} \right\rangle \right\}$$

and

$$\sigma_{f_i} = \left\langle (\delta f_i)^2 \right\rangle^{1/2} .$$

Because of space limitations we have not provided the entire error matrices.

IX. PRODUCTION AMPLITUDES

We have thus far investigated our reaction by using probability distributions. More basic, however, are the quantum-mechanical amplitudes that characterize the production mechanism. The amplitudes, which have been discussed by Byers and Yang,[2] essentially characterize the reaction's behavior in spin space. It will be convenient to normalize our amplitudes so that the probability density one obtains by squaring them corresponds to the $\{f_i\}$ previously defined. If one wants to include factors such as cross sections, flux, or isospin, one's procedure should be straightforward, given s, t, and the cross sections already tabulated. We define our amplitudes $a_{ij}(s,t)$ using state vectors. We note that since the initial proton is unpolarized we have two incoherent amplitudes--for initial proton spin up and down. We quantize with respect to the normal to the production plane, which is the z axis.

$$|\text{initial proton spin up}\rangle \rightarrow \text{final state} = |\text{up}\rangle = a_{--}|--\rangle + a_{+-}|+-\rangle + a_{0+}|0+\rangle$$

$$|\text{initial proton spin down}\rangle \rightarrow \text{final state} = |\text{down}\rangle = a_{++}|++\rangle + a_{-+}|-+\rangle + a_{0-}|0-\rangle$$

$$\text{Probability density} = \langle \text{up}|\text{up}\rangle + \langle \text{down}|\text{down}\rangle$$

$|ij\rangle$ = state with ω-spin projection i and Λ-spin projection j.

Parity conservation, in the form of Bohr's theorem,[6] requires that $|++\rangle$, $|-+\rangle$, and $|0-\rangle$ do not appear in $|\text{up}\rangle$ and that $|--\rangle$, $|+-\rangle$, and $|0+\rangle$ do not appear in $|\text{down}\rangle$.

Let $a_{ij} = |a_{ij}|e^{i\phi_{ij}}$

$$\langle k\ell|ij\rangle = \langle k|i\rangle_\omega \langle \ell|j\rangle_\Lambda$$

<u>ω dependence</u>

$$\langle + | + \rangle_\omega = \frac{1}{2}\left[(\underset{\sim}{n}\cdot \underset{\sim}{X})^2 + (\underset{\sim}{n}\cdot \underset{\sim}{Y})^2 \right]$$

$$\langle + | 0 \rangle_\omega = \langle 0 | + \rangle_\omega^* = -\frac{1}{\sqrt{2}} (\underset{\sim}{n}\cdot \underset{\sim}{N}) \left[(\underset{\sim}{n}\cdot \underset{\sim}{X}) - i(\underset{\sim}{n}\cdot \underset{\sim}{Y}) \right]$$

$$\langle + | - \rangle_\omega = \langle - | + \rangle_\omega^* = -\frac{1}{2}\left[(\underset{\sim}{n}\cdot \underset{\sim}{X})^2 - (\underset{\sim}{n}\cdot \underset{\sim}{Y})^2 - 2i(\underset{\sim}{n}\cdot \underset{\sim}{X})(\underset{\sim}{n}\cdot \underset{\sim}{Y}) \right]$$

$$\langle 0 | 0 \rangle_\omega = (\underset{\sim}{n}\cdot \underset{\sim}{N})^2$$

$$\langle 0 | - \rangle_\omega = \langle - | 0 \rangle_\omega^* = \frac{1}{\sqrt{2}} (\underset{\sim}{n}\cdot \underset{\sim}{N}) \left[(\underset{\sim}{n}\cdot \underset{\sim}{X}) - i(\underset{\sim}{n}\cdot \underset{\sim}{Y}) \right]$$

$$\langle - | - \rangle_\omega = \frac{1}{2}\left[(\underset{\sim}{n}\cdot \underset{\sim}{X})^2 + (\underset{\sim}{n}\cdot \underset{\sim}{Y})^2 \right]$$

<u>Λ dependence</u>

$$\langle + | + \rangle = 1 + \alpha (\underset{\sim}{\pi}\cdot \underset{\sim}{N})$$

$$\langle + | - \rangle = \langle - | + \rangle^* = \alpha \left[(\underset{\sim}{\pi}\cdot \underset{\sim}{X}') + i(\underset{\sim}{\pi}\cdot \underset{\sim}{Y}') \right]$$

$$\langle - | - \rangle = 1 - \alpha (\underset{\sim}{\pi}\cdot \underset{\sim}{N}).$$

The spin-density matrix may be expressed in the following way:

$$\text{Probability density} = \sum_{ijk\ell} \rho_{(ij)(k\ell)} \langle ij | k\ell \rangle ,$$

where the subscripts $(k\ell)$ refer to the initial state and (ij) to the final state, and ρ is the spin-density matrix. From the foregoing equations it is clear that we can express ρ in terms of the amplitudes. See Fig. 7.

Since we already have a method for searching out the $\{f_i\}$ by forming the probability density in terms of the $\{f_i\}$ (see Eq. 1), we can use the same method by forming the probability density as a function of the a_{ij}. In this case we form only one likelihood for each region of s and t that includes the effect of background

$$\ln \mathcal{L} = \sum_{\omega \text{ region}}^{N} \ln P_k - \frac{N_B}{N_C} \sum_{\substack{\text{control} \\ \text{region}}}^{M} \ln P_k .$$

Whereas when we determined the $\{f_i\}$, all we assumed was that the ω indeed has spin 1, and the Λ has spin 1/2; in determining the amplitudes for a particular region of s and t, we are assuming that the phases between the amplitudes do not vary to a great degree over the region of s and t.

Since the above likelihood is not a linear function of the a_{ij}, it does not necessarily have only one maximum. Our search has shown only one maximum in the physical region of the a_{ij} for each of the three regions of s and t that were treated.

We tabulate the amplitudes for three regions of s and t where about 70% of our data happen to be (Table V). We then give the $\{f_i\}$ that correspond to these amplitudes; that is, if one has the amplitudes for the reaction, one can certainly determine the true $\{f_i\}$. These may be compared with the $\{f_i\}$ determined directly, without the assumption that an "amplitude" over a region of s and t is a valid concept (Table VI). The two sets agree within errors. There are six amplitudes; one overall phase is arbitrary (we set a_{--} real), and one phase cannot be determined because we use an unpolarized target (we set a_{++} real). The phases of a_{+-} and a_{0+} are determined with respect to a_{--}. The phases of a_{-+} and a_{0-} are

determined with respect to a_{++}.

The two sets of three amplitudes (one from each spin orientation of the target proton) are presented in graphical form in Fig. 8.

In a later publication we will present amplitudes for other regions of s and t.

X. MOMENTUM-TRANSFER DISTRIBUTIONS

In tabulating t-channel data, we have taken rather large intervals of t in order to deal with a group of events large enough to determine the $\{f_i\}$ in a meaningful way. (We hope.) However, we may be interested only in the momentum-transfer dependence, regardless of the decay angular distributions. Therefore we will provide tables of numbers of events in various s and t intervals, and also plot the momentum-transfer distributions at various values of s (Table VII and Fig. 3).

P_{K^-} = lab momentum of the incident K^-

s = central value of s. Errors represent half widths at half maxima of the distributions in s

$\sigma(s)$ = cross section of $Kp \to \Lambda\omega \to \Lambda\, \pi^+\pi^-\pi^0$ at the indicated s (see Sec. XI)

N(s) = number of $Kp \to \Lambda\omega \to (p\pi^-)(\pi^+\pi^-\pi^0)$ seen in our experiment at the indicated s

N(s,t) = number of $Kp \to \Lambda\omega \to (p\pi^-)(\pi^+\pi^-\pi^0)$ seen in our experiment at the indicated s and between t and $[t - 0.02\ (\mathrm{BeV})^2]$

XI. TOTAL CROSS SECTIONS

In the last section we integrated the cross sections over decay angles, leaving differential cross sections. Here we go one step further and integrate over the momentum transfer squared t, leaving the total cross section, now a function of s only.

It is, of course, true that the actual numbers in the experiment are obtained in the reverse order: One finds the total cross section and then the fractional cross section in any subset. The order of the sections is in the interest of clarity, not chronology.

The $\sigma(s)$ tabulated in Sec. VII were found by averaging the cross sections obtained here over the region of s treated.

A. $Kp \rightarrow \Lambda \pi^+\pi^-\pi^0$

Total cross sections for $Kp \rightarrow \Lambda \pi^+\pi^-\pi^0$ in our experiment have been determined by Huwe.[7] The values are listed in Table I.

By making two corrections, we have gone one step further in determining total cross sections. The first problem in need of correction arises from studying those events that were found by our scanning the film but which were not measured at all, either due to an oversight or because the measurer felt there was something wrong with them. In his calculations, Huwe assumed that these events were good events, distributed among the various reactions in the same way as the events that went through the entire analyzing system. In order to check this assumption, we scanned a sample of events at each momentum to analyze the causes of rejection. Small corrections to the cross sections resulted from this refinement, but the correction was of significance at only one momentum--1.5 BeV/c. The second problem arises from the Dalitz decay of the π^0. The π^0 from

$\omega \rightarrow \pi^+\pi^-\pi^0$ decay will give a Dalitz pair 1.25% of the time. There would then be four prongs at the production vertex, and since we looked only at V + two-prongs we must increase each cross section by 1.25% to account for this effect. The corrected cross sections are also listed in Table I.

Huwe treated all V + two-prong events in the experiment except those in the sample at 1.52 BeV/c, where he analyzed about one-half the total.[7] The second half was analyzed completely independently by methods essentially the same, except for the treatment of events that were measured but failed to fit any hypothesis. In this sample there were 1270 such events. Twenty events were selected at random and separately analyzed by the program QUEST. The results of this analysis showed that the 20 events were consistent with being:

2	$Kp \rightarrow$	$\Lambda\ \pi^+\pi^-\pi^0$	1	$\bar{K}^0\pi^+\pi^-n$
6		$\Lambda\ \pi^+\pi^-$	2	K^-p
2		$\Lambda\ \pi^0$	1	$K^-p\pi^0$
4		$\bar{K}^0\ p\pi^-$	2	$K^-\pi^+n$

The reasons for their failure were:

6	track scatter
2	bad measurement
2	the two-prong at the production vertex or the V is an e^+e^- pair
1	secondary interaction
3	V doesn't go with the production vertex
6	bubble chamber problems

B. $\underline{Kp \rightarrow \Lambda\omega \rightarrow \Lambda\pi^+\pi^-\pi^0}$

We have samples of events that satisfy $Kp \rightarrow \Lambda\pi^+\pi^-\pi^0$. At each momentum we plot the three-pion effective-mass spectrum. In each case the η and the ω show prominently. By sketching a background curve we can estimate the amount of ω actually in the sample, as we did in Sec. VI. We took the number of events above the background curve and between 750 and 815 MeV to represent the number of ω's in each case. The background curves we drew do not fit phase space very well. The distributions with the background curves are shown in Fig. 1. The cross sections are graphed in Fig. 2.

XII. REMARKS ON THEORETICAL MODELS

A. Resonance Formation–s-Channel Dominance

The data would have certain distinctive characteristics if a strong $Y = 0$, $T = 0$ resonance were coupled to both the K^-p and the $\Lambda\omega$ channels with a mass squared in the region of s where our data fall: (a) The total cross section would have a peak whose position and width would correspond to the mass and width of the resonance. (b) The distribution in production angle at a given s would reflect the angular-momentum states into which the resonance decays. (c) The decay angular distributions of the Λ and ω would also reflect the states of angular momentum into which the resonance decays.

The total-cross-section curve exhibits no obvious enhancements in the region where our data lie, except for the broad peak associated with threshold. The distributions in t, which correspond to distributions in angle, show no striking behavior as a function of energy, and although the distributions do not require high angular-momentum states for their explanation, neither do they isolate any one angular-momentum state as being dominant.

Thus the only comment that can be made about s-channel activity (resonance formation) with the amount of data available is that this activity is not an overpowering feature in determining the reaction's production characteristics.

B. Meson-Exchange Model–t-Channel Dominance

The exchange of $Y = -1$, $T = 1/2$ systems in the t channel [see Fig. 4(b)] is a possible production mechanism in $Kp \rightarrow \Lambda\omega$. The data would reveal the dominance of such a process in two areas. (a) The distribution in t would reflect the propagators of the exchanged particles as well as

effects from spin, absorption, and form factors. Our distributions in t below s = 4.1 $(\mathrm{BeV})^2$ exhibit a feature common to many quasi-two-body reactions—that is, the peaking toward lower t is even more pronounced than the exchange of the lightest possible particle would predict (see Fig. 3). We have not included absorption in the model. It is commonly accepted that such a momentum-transfer distribution could be explained by refinements such as absorption or an arbitrary form factor, and therefore, despite the comparison in Fig. 8, the exchange model may still be applicable. (b) A more stringent test of the exchange model is the comparison between its predictions of decay angular correlations and the data. We list here the various predictions given by the simple exchange model without absorptive corrections. Comparison with the tabulated data shows that none of the listed possibilities satisfy the data. The most significant comparison would be with low-momentum-transfer regions. The phrase "not exhaustive" after a prediction means that the listed equations are required by the model, but that other relationships, which are not listed, are also predicted by the model.

i. 0^- exchange (e.g., K): All $f_i = 0$ except f_2.

ii. 1^- (e.g., K^*): All $f_i = 0$ except f_1 and f_3.

iii. 0^- and 1^-: $f_4 = f_6 = f_7 = f_{10} = 0$.

With the additional assumption that the two coupling constants for the vector exchange are relatively real, we get

$$f_5 = f_{12} = 0.$$

With the additional assumption that the pseudoscalar exchange coupling constant and the vector coupling constants are relatively real, we get $f_8 = f_9 = f_{11} = 0$.

iv. any combination of normal parity exchanges (0^+, 1^-, 2^+, $\cdots$)

$f_2 = f_4 = 0$ (not exhaustive).

C. Baryon Exchange Model–u-Channel Dominance

i. $\frac{1}{2}^+$ or $\frac{1}{2}^-$ exchange: $f_5 = 0$, $f_1 = f_3$ (not exhaustive).

If coupling constants are relatively real, then

$$f_6 = f_7 = f_8 = f_9 = f_{10} = f_{11} = f_{12} = 0.$$

Thus we see that there is no obvious resonance in the s channel indicated by our data, and that simple exchange models in the t and u channels do not fit the data. We have not yet embarked upon an investigation of the absorption model.[8]

ACKNOWLEDGMENTS

We thank Professor Luis W. Alvarez, Dr. Robert Huff, Professor Samuel M. Berman, and Dr. C. N. Yang for their interest and motivating discussion. We also thank the members of the scanning and measuring group for their important contributions to this work.

FOOTNOTES AND REFERENCES

*Work done under the auspices of the U. S. Atomic Energy Commission.

†National Science Foundation Predoctoral Fellow.

1. S. M. Flatté, D. O. Huwe, J. J. Murray, J. B. Shafer, F. T. Solmitz, M. Lynn Stevenson, and C. Wohl, Decay Properties of the ω Meson, Lawrence Radiation Laboratory Report UCRL-16443 (unpublished); submitted to Phys. Rev.
2. N. Byers and C. N. Yang, Phys. Rev. 135, B796 (1964).
3. S. M. Berman and R. J. Oakes, Phys. Rev. 135, B1034 (1964).
4. R. W. Huff, Phys. Rev. 133, B1078 (1964).
5. M. Ademollo and R. Gatto, Phys. Rev. 133, B531 (1964).
6. A. Bohr, Nuclear Physics 10, 486-491 (1959).
7. D. O. Huwe, Study of the Reaction $K^- + p \rightarrow \Lambda + \pi^+ + \pi^-$ from 1.2 to 1.7 BeV/c (Ph. D. thesis), Lawrence Radiation Laboratory Report UCRL-11291 (1964) (unpublished).
8. J. D. Jackson, Rev. Mod. Phys. 37, 484 (1965).

Table I. Path lengths and cross sections for $K^-p \rightarrow \Lambda \pi^+\pi^-\pi^0$ and $K^-p \rightarrow \Lambda \omega$.

	Momentum (BeV/c)							
	1.22	1.32	1.42	1.51(I)	1.51(II)	1.51	1.60	1.69
$s(\mathrm{BeV})^2$	3.58	3.77	3.91	4.08	4.08	4.08	4.24	4.42
Total path length (events/mb)	1230±60	1440±70	825±40	2600±100	2500±100	5085±200	715±35	1100±55
$\sigma(Kp \rightarrow \Lambda\pi^+\pi^-\pi^0)$[a] (mb)	0.68±0.05	1.51±0.10	2.12±0.06	2.47±0.12			2.19±0.15	2.83±0.17
$\sigma(Kp \rightarrow \Lambda\pi^+\pi^-\pi^0)$ revised (mb)	0.68±0.05	1.53±0.10	2.10±0.06	2.35±0.12	2.18±0.10	2.26±0.08	2.14±0.15	2.82±0.17
$N(\pi^+\pi^-\pi^0)$	392	965	1093	2843	3004	5847	1006	1000
$N(\omega \rightarrow \pi^+\pi^-\pi^0)$	0±30	502	505	1202	1273	2475	366	357
$\sigma(Kp \rightarrow \Lambda\omega \rightarrow \Lambda\pi^+\pi^-\pi^0)$ (mb)	0±0.05	0.80±0.06	0.97±0.08	0.99±0.07	0.93±0.07	0.96±0.05	0.78±0.05	1.01±0.06

[a]See Ref. 7

Table II. Data for t channel. $\underset{\sim}{X} = \underset{\sim}{q}_1$ $\underset{\sim}{X}' = \underset{\sim}{P}_1$

$s_{min}(BeV)^2$	3.55		3.91			4.27		
$s_{max}(BeV)^2$	3.91		4.27			4.63		
$\sigma(s)$ (mb)	0.66 ± 0.04		0.91 ± 0.05			1.01 ± 0.06		
N(s)	1041		3843			761		
$t_{min}(BeV)^2$	-0.436	-0.757	-0.436	-0.757	-1.24	-0.436	-0.757	-1.6
$t_{max}(BeV)^2$	-0.170	-0.436	-0.10	-0.436	-0.757	-0.04	-0.436	-0.757
N(s,t)	624	397	1729	1419	696	226	204	331
BG(s,t)	117	117	381	436	273	59	29	101
$\frac{d\sigma}{dt}$ mb/(BeV)^2	1.19 ± 0.08	0.55 ± 0.04	0.94 ± 0.05	0.73 ± 0.04	0.21 ± 0.02	0.55 ± 0.08	0.73 ± 0.08	0.32 ± 0.05
f_1	0.302 ± 0.039	0.306 ± 0.059	0.234 ± 0.022	0.239 ± 0.030	0.431 ± 0.055	0.255 ± 0.069	0.308 ± 0.063	0.427 ± 0.065
f_2	0.425 ± 0.041	0.522 ± 0.061	0.507 ± 0.023	0.588 ± 0.032	0.354 ± 0.054	0.628 ± 0.072	0.617 ± 0.061	0.451 ± 0.064
f_3	0.272 ± 0.037	0.172 ± 0.052	0.259 ± 0.022	0.188 ± 0.030	0.215 ± 0.053	0.117 ± 0.058	0.075 ± 0.055	0.123 ± 0.057
f_4	0.368 ± 0.063	0.449 ± 0.094	0.334 ± 0.038	0.411 ± 0.053	0.231 ± 0.093	0.367 ± 0.123	0.324 ± 0.098	0.240 ± 0.109
f_5	-0.089 ± 0.071	0.091 ± 0.110	-0.106 ± 0.039	-0.030 ± 0.057	0.278 ± 0.105	-0.078 ± 0.129	-0.060 ± 0.116	-0.132 ± 0.128
f_6	-0.191 ± 0.077	-0.068 ± 0.115	-0.153 ± 0.045	-0.205 ± 0.065	-0.050 ± 0.103	-0.012 ± 0.157	-0.094 ± 0.144	-0.168 ± 0.132
f_7	0.088 ± 0.062	-0.036 ± 0.094	0.063 ± 0.041	0.078 ± 0.053	-0.159 ± 0.096	0.134 ± 0.128	0.008 ± 0.092	0.048 ± 0.098
f_8	-0.256 ± 0.108	-0.082 ± 0.168	-0.309 ± 0.066	-0.232 ± 0.092	-0.416 ± 0.157	-0.611 ± 0.226	-0.220 ± 0.181	-0.001 ± 0.193
f_9	-0.027 ± 0.112	0.085 ± 0.178	0.268 ± 0.073	-0.047 ± 0.098	-0.065 ± 0.175	0.369 ± 0.218	0.005 ± 0.216	-0.287 ± 0.200
f_{10}	-0.098 ± 0.120	0.133 ± 0.168	-0.107 ± 0.069	-0.135 ± 0.086	0.223 ± 0.167	0.076 ± 0.214	-0.219 ± 0.156	-0.047 ± 0.178
f_{11}	-0.050 ± 0.111	0.439 ± 0.179	-0.124 ± 0.067	0.088 ± 0.097	0.254 ± 0.167	0.005 ± 0.204	-0.030 ± 0.186	0.447 ± 0.190
f_{12}	0.427 ± 0.107	+0.437 ± 0.165	0.111 ± 0.061	0.211 ± 0.084	0.183 ± 0.160	0.199 ± 0.193	0.115 ± 0.153	0.222 ± 0.173

Table III. Data for u channel. $\underset{\sim}{X} = P_1$ $\underset{\sim}{X}' = \underset{\sim}{q}_1$

$s_{min}(BeV)^2$	3.55		3.91			4.27		
$s_{max}(BeV)^2$	3.91		4.27			4.63		
$\sigma(s)(mb)$	0.66 ± 0.04		0.91 ± 0.05			1.01 ± 0.06		
N(s)	1041		3843			761		
$u_{min}(BeV)^2$	-0.341	-0.658	-0.341	-0.658	-0.98	-0.341	-0.658	-1.61
$u_{max}(BeV)^2$	-0.12	-0.341	-0.06	-0.341	-0.658	-0.06	-0.341	-0.658
N(s, u)	399	609	720	1438	1682	166	163	430
BG(s, u)	130	143	388	481	390	65	39	111
$\frac{d\sigma}{du}$ mb/(BeV)^2	0.78 ± 0.06	0.92 ± 0.07	0.44 ± 0.04	0.71 ± 0.04	0.96 ± 0.05	0.48 ± 0.05	0.51 ± 0.05	0.45 ± 0.05
f_1	0.327 ± 0.061	0.258 ± 0.044	0.413 ± 0.060	0.209 ± 0.031	0.243 ± 0.024	0.657 ± 0.110	0.241 ± 0.074	0.279 ± 0.052
f_2	0.584 ± 0.061	0.561 ± 0.045	0.315 ± 0.057	0.470 ± 0.032	0.495 ± 0.026	-0.058 ± 0.093	0.382 ± 0.077	0.322 ± 0.050
f_3	0.089 ± 0.053	0.181 ± 0.039	0.272 ± 0.060	0.322 ± 0.031	0.263 ± 0.024	0.401 ± 0.105	0.377 ± 0.079	0.399 ± 0.051
f_4	-0.455 ± 0.102	-0.007 ± 0.075	-0.302 ± 0.100	-0.578 ± 0.054	-0.255 ± 0.045	-0.327 ± 0.163	-0.442 ± 0.142	-0.590 ± 0.084
f_5	-0.043 ± 0.114	-0.044 ± 0.082	0.321 ± 0.113	-0.034 ± 0.059	-0.131 ± 0.045	-0.174 ± 0.223	-0.098 ± 0.145	-0.059 ± 0.094
f_6	-0.101 ± 0.120	-0.171 ± 0.090	-0.278 ± 0.108	-0.160 ± 0.061	-0.202 ± 0.052	0.170 ± 0.173	0.004 ± 0.137	-0.113 ± 0.093
f_7	0.098 ± 0.108	0.054 ± 0.067	0.224 ± 0.113	-0.043 ± 0.057	0.119 ± 0.045	-0.079 ± 0.208	-0.066 ± 0.173	-0.000 ± 0.106
f_8	-0.056 ± 0.175	0.143 ± 0.120	0.218 ± 0.170	0.336 ± 0.093	0.041 ± 0.078	-0.213 ± 0.294	0.043 ± 0.262	0.197 ± 0.159
f_9	0.022 ± 0.195	0.138 ± 0.132	0.376 ± 0.171	-0.033 ± 0.096	0.150 ± 0.077	0.308 ± 0.294	-0.123 ± 0.247	0.150 ± 0.151
f_{10}	0.127 ± 0.175	0.062 ± 0.116	0.196 ± 0.182	-0.065 ± 0.098	-0.122 ± 0.077	-0.344 ± 0.323	0.060 ± 0.262	-0.016 ± 0.157
f_{11}	0.506 ± 0.187	0.153 ± 0.140	0.303 ± 0.184	0.238 ± 0.096	-0.106 ± 0.077	0.353 ± 0.256	0.242 ± 0.242	0.073 ± 0.143
f_{12}	$+0.178 \pm 0.181$	0.321 ± 0.119	-0.293 ± 0.177	-0.018 ± 0.093	0.341 ± 0.074	1.10 ± 0.287	0.171 ± 0.250	0.133 ± 0.153

Table IV. Data for s channel. $\underset{\sim}{X} = \underset{\sim}{P}_2$ $\underset{\sim}{X}' = \underset{\sim}{q}_2$

$s_{min}(BeV)^2$	3.55	3.91	4.03	4.15	4.27
$s_{max}(BeV)^2$	3.91	4.03	4.15	4.27	4.63
$\sigma(s)$(mb)	0.66 ± 0.04	0.96 ± 0.05	0.92 ± 0.05	0.84 ± 0.05	1.01 ± 0.06
N(s)	1041	1021	2083	739	761
BG(s)	286	296	604	214	182
f_1	0.311 ± 0.036	0.199 ± 0.035	0.278 ± 0.025	0.274 ± 0.041	0.347 ± 0.038
f_2	0.252 ± 0.034	0.310 ± 0.037	0.206 ± 0.024	0.202 ± 0.039	0.175 ± 0.035
f_3	0.438 ± 0.037	0.492 ± 0.037	0.516 ± 0.026	0.524 ± 0.042	0.477 ± 0.038
f_4	-0.162 ± 0.059	-0.088 ± 0.062	-0.118 ± 0.044	-0.107 ± 0.072	0.032 ± 0.065
f_5	-0.043 ± 0.066	0.013 ± 0.063	-0.047 ± 0.046	-0.110 ± 0.076	-0.078 ± 0.072
f_6	0.037 ± 0.063	0.016 ± 0.068	0.013 ± 0.044	-0.041 ± 0.074	-0.030 ± 0.065
f_7	-0.108 ± 0.066	-0.223 ± 0.070	-0.082 ± 0.051	-0.022 ± 0.084	-0.032 ± 0.079
f_8	0.132 ± 0.103	0.249 ± 0.104	0.141 ± 0.075	-0.024 ± 0.125	0.035 ± 0.114
f_9	0.281 ± 0.101	-0.048 ± 0.104	0.084 ± 0.072	-0.002 ± 0.119	0.032 ± 0.101
f_{10}	-0.063 ± 0.104	-0.107 ± 0.112	-0.005 ± 0.078	-0.077 ± 0.127	-0.167 ± 0.109
f_{11}	0.025 ± 0.107	-0.111 ± 0.104	0.055 ± 0.074	0.095 ± 0.116	0.053 ± 0.112
f_{12}	0.227 ± 0.108	0.139 ± 0.110	0.334 ± 0.079	0.071 ± 0.125	0.151 ± 0.120

Table V. Production amplitudes.[a]
Region of s: 3.91 to 4.26 $(BeV)^2$.

t_{min} $(BeV)^2$	-0.436	-0.757	-1.03
t_{max} $(BeV)^2$	-0.117	-0.436	-0.757
$\|a_{--}\|$	0.292	0.293	0.028
$\|a_{+-}\|$	0.047 ± 0.032	0.027 ± 0.134	0.246 ± 0.026
ϕ_{+-}	-1.09 ± 0.088	-3.99 ± 0.047	-0.81 ± 0.022
$\|a_{0+}\|$	0.236 ± 0.021	0.207 ± 0.024	0.005 ± 0.027
ϕ_{0+}	-1.61 ± 0.089	-0.96 ± 0.387	-2.20 ± 0.034
$\|a_{++}\|$	0.276 ± 0.049	0.278 ± 0.019	0.327 ± 0.024
$\|a_{-+}\|$	0.308 ± 0.048	0.305 ± 0.017	0.157 ± 0.021
ϕ_{-+}	-2.21 ± 0.073	-2.37 ± 0.105	-2.06 ± 0.034
$\|a_{0-}\|$	0.139 ± 0.030	0.180 ± 0.110	0.376 ± 0.013
ϕ_{0-}	-5.57 ± 0.084	-4.71 ± 0.053	-4.12 ± 0.030

Table VI. Comparison of $\{f_i\}$ determined directly and $\{f_i\}$ determined from the amplitudes in Table V.

$t_{min}(BeV)^2$	-0.436		-0.757		-1.03	
$t_{max}(BeV)^2$	-0.117		-0.436		-0.757	
	Amp. f_i	Direct f_i	Amp. f_i	Direct f_i	Amp. f_i	Direct f_i
f_1	0.226	0.234 ± 0.022	0.226	0.239 ± 0.030	0.424	0.431 ± 0.055
f_2	0.520	0.507 ± 0.023	0.586	0.588 ± 0.032	0.346	0.354 ± 0.054
f_3	0.254	0.259 ± 0.022	0.188	0.188 ± 0.030	0.230	0.215 ± 0.053
f_4	0.335	0.334 ± 0.038	0.392	0.411 ± 0.053	0.242	0.231 ± 0.093
f_5	-0.067	-0.105 ± 0.039	-0.020	-0.030 ± 0.057	0.263	0.278 ± 0.105
f_6	-0.183	-0.153 ± 0.045	-0.182	-0.205 ± 0.065	-0.119	-0.050 ± 0.103
f_7	0.030	0.063 ± 0.041	0.025	0.078 ± 0.053	-0.117	-0.159 ± 0.096
f_8	-0.299	-0.309 ± 0.066	-0.199	-0.232 ± 0.092	-0.186	-0.416 ± 0.157
f_9	-1.218	0.268 ± 0.073	-0.005	-0.047 ± 0.098	-0.106	-0.065 ± 0.175
f_{10}	-0.105	-0.107 ± 0.069	-0.101	-0.135 ± 0.086	0.127	0.223 ± 0.167
f_{11}	-0.124	-0.124 ± 0.067	0.103	0.088 ± 0.097	0.408	0.254 ± 0.167
f_{12}	0.053	0.111 ± 0.061	0.178	0.211 ± 0.084	0.253	0.183 ± 0.160

Table VII. Distributions of t in $K^-p \rightarrow \Lambda\omega$ for K^- momenta between 1.2 and 1.8 BeV/c. Background has been subtracted.

	Momenta of K^-				
	1.32	1.42	1.50	1.60	1.69
$s(BeV)^2$	3.77 ± 0.08	3.91 ± 0.09	4.08 ± 0.08	4.24 ± 0.10	4.42 ± 0.09
$\sigma(s)$(mb)	0.80 ± 0.06	0.97 ± 0.08	0.96 ± 0.05	0.78 ± 0.05	1.01 ± 0.06
N(s)	502	505	2475	366	357
t	N(s,t)	N(s,t)	N(s,t)	N(s,t)	N(s,t)
-0.10	-3 ± 3	-3 ± 3	4 ± 3	4 ± 2	7 ± 3
-0.12	-3 ± 3	3 ± 3	42 ± 7	5 ± 2	9 ± 3
-0.14	-5 ± 3	5 ± 4	85 ± 9	7 ± 3	8 ± 3
-0.16	4 ± 3	14 ± 4	90 ± 10	5 ± 3	2 ± 3
-0.18	6 ± 3	14 ± 4	81 ± 10	5 ± 3	7 ± 4
-0.20	6 ± 5	16 ± 4	89 ± 11	7 ± 4	7 ± 3
-0.22	35 ± 6	6 ± 4	61 ± 10	2 ± 3	7 ± 3
-0.24	23 ± 6	13 ± 4	79 ± 11	6 ± 3	6 ± 3
-0.26	31 ± 6	14 ± 4	87 ± 11	10 ± 4	13 ± 4
-0.28	31 ± 6	15 ± 4	79 ± 11	5 ± 3	13 ± 4
-0.30	39 ± 7	19 ± 5	66 ± 11	3 ± 3	7 ± 4
-0.32	37 ± 7	11 ± 4	86 ± 12	5 ± 3	5 ± 3
-0.34	34 ± 7	23 ± 5	68 ± 11	5 ± 3	9 ± 3
-0.36	31 ± 7	22 ± 5	84 ± 11	7 ± 3	4 ± 3
-0.38	31 ± 7	14 ± 5	75 ± 11	8 ± 3	3 ± 4
-0.40	17 ± 6	22 ± 5	85 ± 11	7 ± 3	6 ± 3
-0.42	24 ± 6	9 ± 5	67 ± 10	2 ± 3	13 ± 4
-0.44	23 ± 4	18 ± 5	81 ± 11	2 ± 3	14 ± 4
-0.46	36 ± 7	13 ± 5	80 ± 11	4 ± 3	9 ± 3
-0.48	18 ± 5	9 ± 4	99 ± 12	4 ± 3	7 ± 3
-0.50	11 ± 5	11 ± 4	76 ± 11	11 ± 3	9 ± 3
-0.52	11 ± 5	8 ± 4	53 ± 10	5 ± 3	8 ± 3
-0.54	5 ± 4	16 ± 5	54 ± 10	-2 ± 2	7 ± 3
-0.56	10 ± 5	1 ± 4	57 ± 10	9 ± 3	3 ± 3
-0.58	23 ± 5	16 ± 4	55 ± 10	4 ± 3	8 ± 3
-0.60	10 ± 4	10 ± 4	43 ± 9	5 ± 3	9 ± 4
-0.62	6 ± 3	11 ± 5	53 ± 9	-3 ± 2	6 ± 3
-0.64	7 ± 4	4 ± 4	50 ± 9	9 ± 3	10 ± 4
-0.66	5 ± 4	8 ± 4	41 ± 9	4 ± 3	6 ± 3
-0.68	8 ± 4	7 ± 3	45 ± 9	2 ± 3	11 ± 4
-0.70	3 ± 4	7 ± 3	45 ± 9	3 ± 3	2 ± 3
-0.72	1 ± 3	2 ± 3	42 ± 9	5 ± 3	6 ± 3
-0.74		7 ± 3	23 ± 8	1 ± 3	9 ± 3
-0.76		-1 ± 3	20 ± 8	1 ± 3	7 ± 3
-0.78		6 ± 3	23 ± 7	6 ± 3	10 ± 4
-0.80		-1 ± 3	44 ± 8	7 ± 3	4 ± 2
-0.82		3 ± 3	27 ± 7	0 ± 2	5 ± 3
-0.84		1 ± 3	26 ± 8	5 ± 3	9 ± 3
-0.86		5 ± 3	34 ± 7	1 ± 3	8 ± 3
-0.88		-1 ± 1	22 ± 7	1 ± 3	7 ± 4
-0.90		-2 ± 2	29 ± 7	2 ± 2	0 ± 2
-0.92		1 ± 2	23 ± 7	5 ± 3	5 ± 3
-0.94			30 ± 8	1 ± 2	1 ± 3
-0.96			14 ± 6	3 ± 3	6 ± 3
-0.98			22 ± 6	3 ± 2	7 ± 3
-1.00			17 ± 5	4 ± 3	13 ± 4
-1.02			18 ± 5	3 ± 2	8 ± 3
-1.04			21 ± 5	4 ± 2	10 ± 4
-1.06			4 ± 4	2 ± 2	6 ± 3
-1.08			0 ± 4	5 ± 2	3 ± 3
-1.10			6 ± 4	2 ± 2	8 ± 4
-1.12			1 ± 4	2 ± 2	8 ± 3
-1.14				1 ± 2	9 ± 4
-1.16				4 ± 2	11 ± 4
-1.18				2 ± 2	4 ± 3
-1.20				3 ± 2	10 ± 3
-1.22				5 ± 2	9 ± 3
-1.24				1 ± 1	3 ± 3
-1.26					10 ± 3
-1.28					3 ± 3
-1.30					4 ± 2
-1.32					4 ± 2
-1.34					5 ± 3
-1.36					7 ± 3
-1.38					4 ± 3
-1.40					5 ± 2
-1.42					3 ± 2
-1.44					0 ± 2
-1.46					1 ± 1
-1.48					-1 ± 1
-1.50					1 ± 2
-1.52					1 ± 1

FIGURE CAPTIONS

Fig. 1. Three-pion mass spectra from $K^-p \rightarrow \Lambda \pi^+ \pi^- \pi^0$ for various incident laboratory momenta. The curves are estimates of the background made by eye. (a) 10130 events; (b) 5848 events; (c) 429 events; (d) 1075 events; (e) 798 events; (f) 644 events; (g) 1336 events.

Fig. 2. Cross sections of the reactions $K^-p \rightarrow \Lambda \pi^+ \pi^- \pi^0$ (top curve) and $K^-p \rightarrow \Lambda + (\omega \rightarrow \pi^+ \pi^- \pi^0)$ (bottom curve) from threshold to 3 BeV/c incident K^- momentum. The connecting lines are to eliminate confusion only.

(a) P. L. Bastien and J. P. Berge, K^-p Interactions near 760 MeV/c, Phys. Rev. Letters 10, 188 (1963).

(b) P. M. Dauber, W. M. Dunwoodie, P. E. Schlein, W. E. Slater, L. T. Smith, D. H. Stork and H. K. Ticho, Exchange Mechanisms in K^-p Reactions at 1.8 and 1.95 GeV/c, presented at the Second Topical Conference on Resonant Particles- Athens, Ohio, June 1965; and L. T. Smith, Ph. D. Thesis, Univ. of Calif., Los Angeles.

(c) P. L. Connolly, E. L. Hart, K. W. Lai, G. London, G. C. Moneti, R. R. Rau, N. P. Samios, I. O. Skillicorn, S. S. Yamamoto, M. Goldberg, M. Gundzik, J. Leitner, and S. Lichtman, Proceedings of the Sienna International Conference on Elementary Particles, (Societa Italiana di Fisica, Bologna, 1963) p. 130.

(d) R. R. Ross, J. H. Friedman, D. M. Siegel, S. Flatté, L. W. Alvarez, A. Barbaro-Galtieri, J. Button-Shafer, O. I. Dahl, P. Eberhard, W. E. Humphrey, G. R. Kalbfleisch, J. S. Lindsey, D. W. Merrill, G. A. Smith, and R. D. Tripp, Production of S = 0, -1 Resonant States in K^-p Interactions at 2.45 GeV/c, 1964 International Conference on High Energy Physics, Dubna, USSR (1964).

(e) E. S. Gelsema, J. C. Kluyver, A. G. Tenner, M. Demoulin, J. Goldberg, B. P. Gregory, G. Kayas, P. Krejbich, C. Pelletier, R. Barloutand, A. Leveque, C. Louedec, J. Meyer, and A. Verglas, Proceedings of the Sienna International Conference on Elementary Particles (Societa Italiana di Fisica, Bologna, 1963) p. 134.

Fig. 3. Distributions in t for center-of-mass energy-squared s between 3.7 and 4.5 BeV^2 for $K^-p \rightarrow \Lambda\omega$. Background has been subtracted.

Fig. 4. Feynman diagrams representing exchanges in the three channels that affect $K^-p \rightarrow \Lambda\omega$. Exchanges of the least massive particles are shown.

Fig. 5. Diagram of $K^-p \rightarrow \Lambda\omega$ with the particles labeled by two symbols; the first is the four-momentum and the second is the mass of the particle.

Fig. 6. Regions of s, t, and u chosen for determination of production parameters. (a) t-channel selections; (b) u-channel selections. The units of s and t are $(BeV)^2$.

Fig. 7. Spin-density matrix ρ in terms of the production amplitudes. The first index of either (i j) or (k l) refers to the ω spin projection along the normal to the production plane, the second to the Λ spin projection. The terms in the solid boxes come from initial states having target-proton-spin projection + 1/2; the other terms come from -1/2. Terms left blank are required to be zero by the conservation of parity.

Fig. 8. The six production amplitudes describing $K^-p \rightarrow \Lambda\omega$ for three regions of t within one region of s. $3.91 < s < 4.26$ $(BeV)^2$; t-channel axes were used.

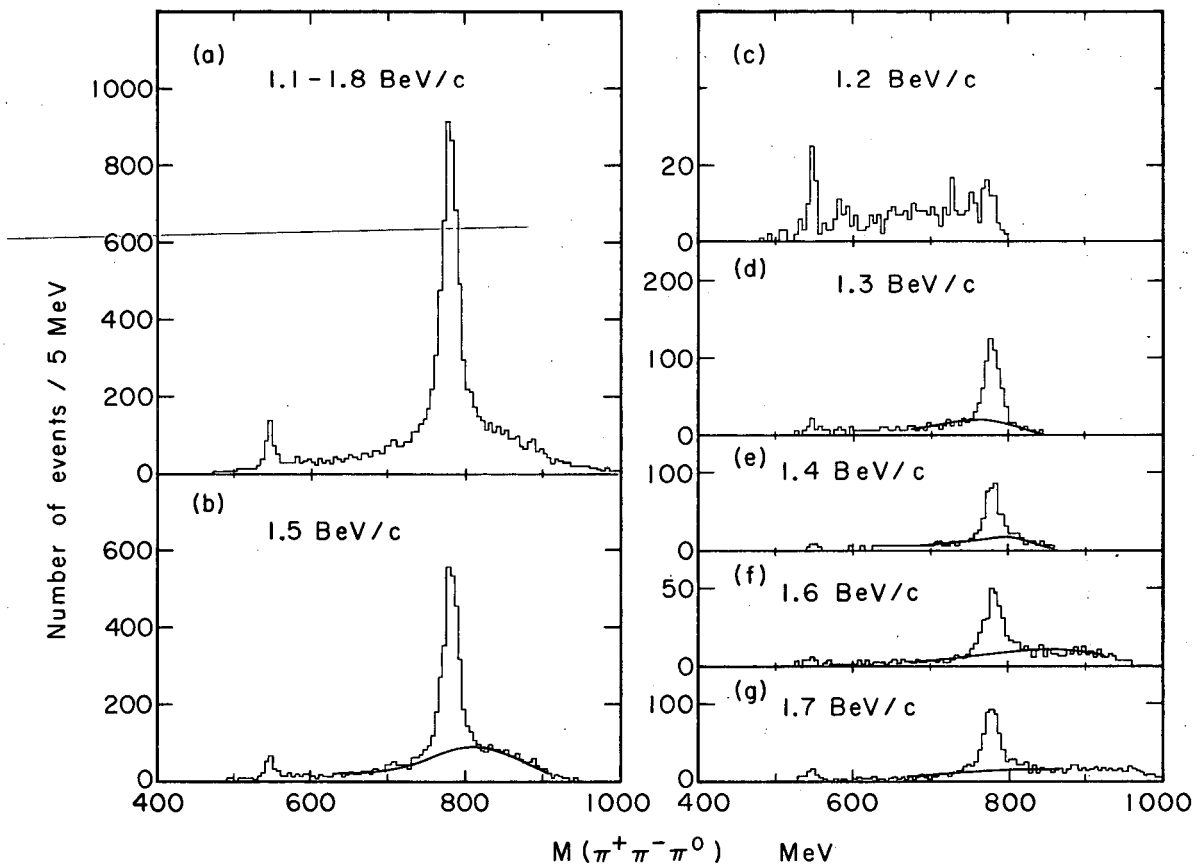
(a)
1.1 - 1.8 BeV/c
(b)
1.5 BeV/c
(c)
1.2 BeV/c
(d)
1.3 BeV/c
(e)
1.4 BeV/c
(f)
1.6 BeV/c
(g)
1.7 BeV/c
Number of events / 5 MeV
M ($\pi^+\pi^-\pi^0$) MeV
MUB-8401

Fig. 1

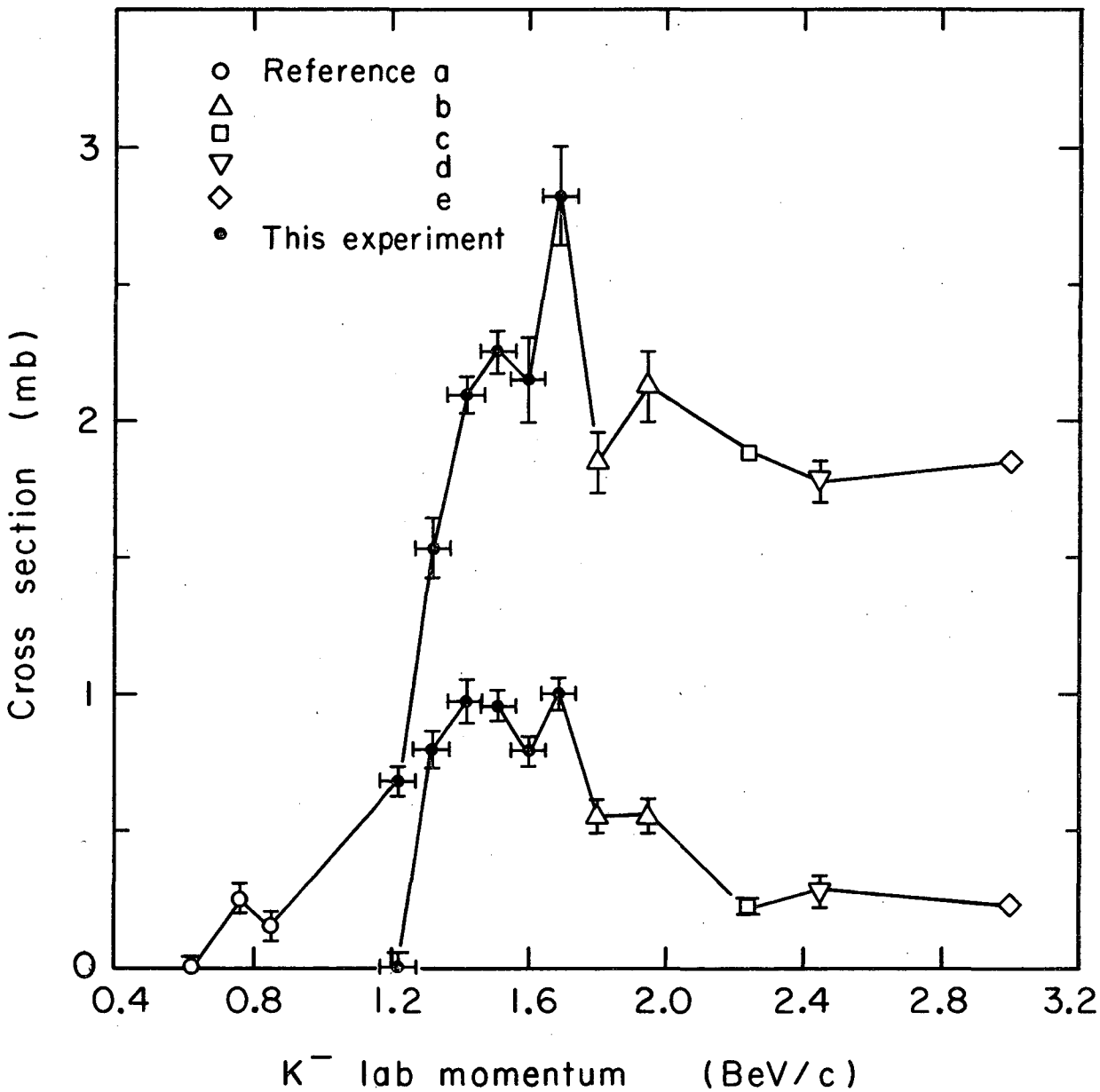

MUB-8402

Fig. 2

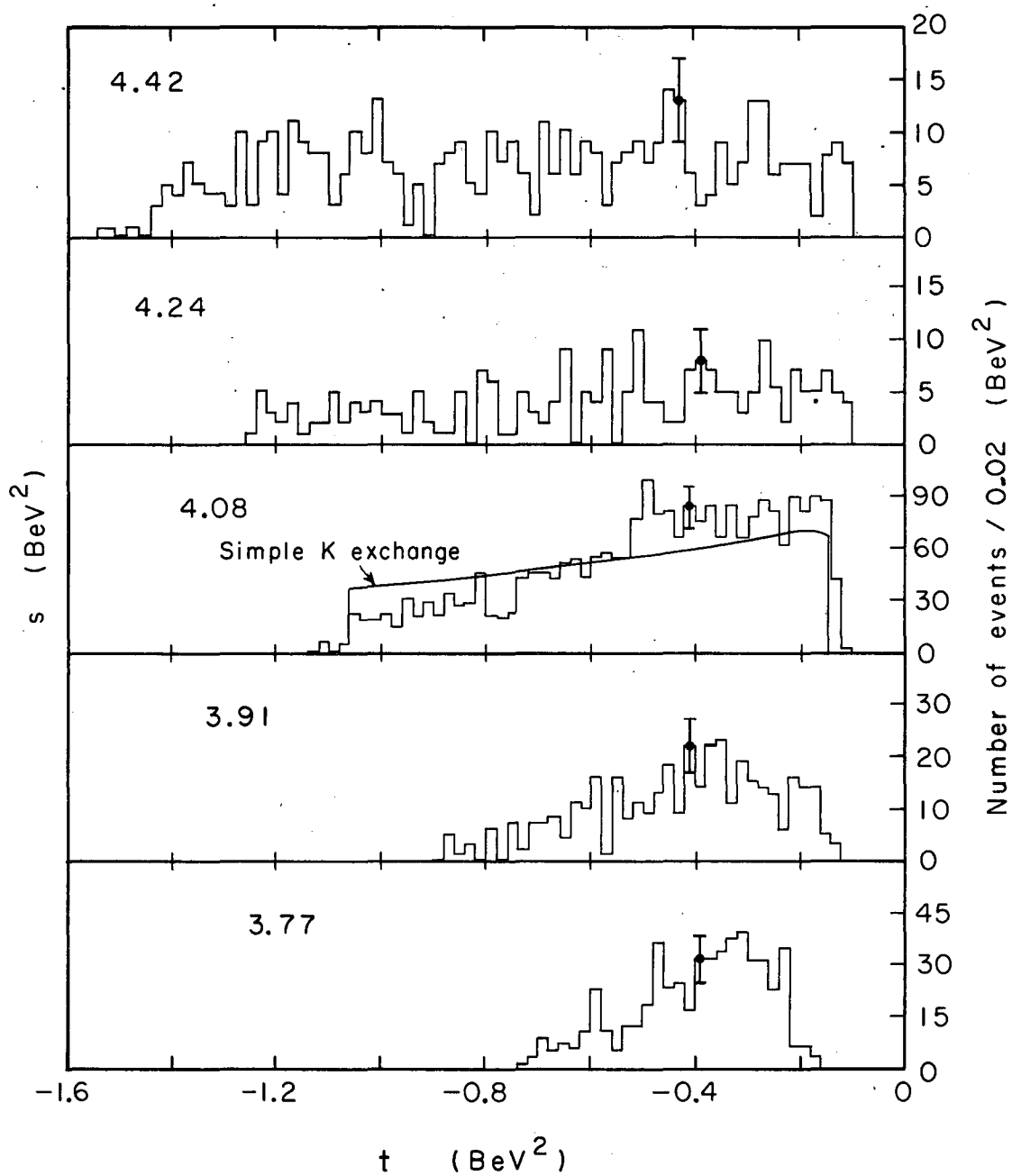

MUB-8403

Fig. 3

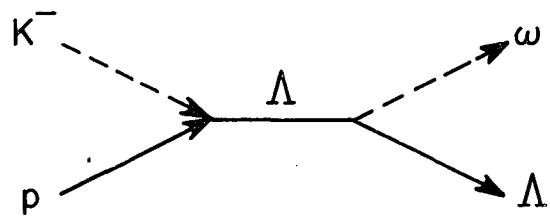

s channel

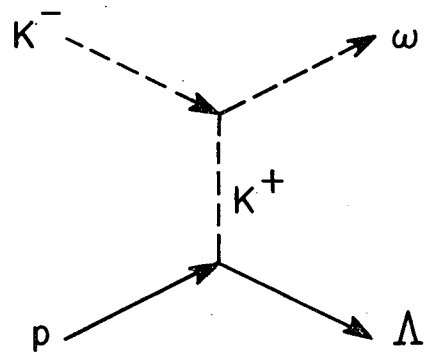

t channel

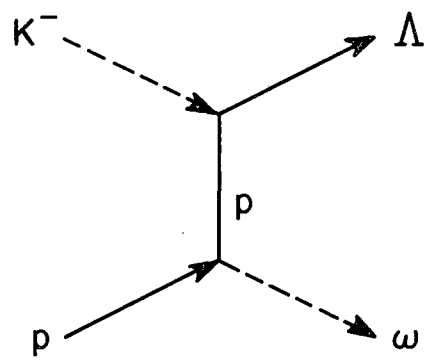

u channel

MUB-8404

Fig. 4

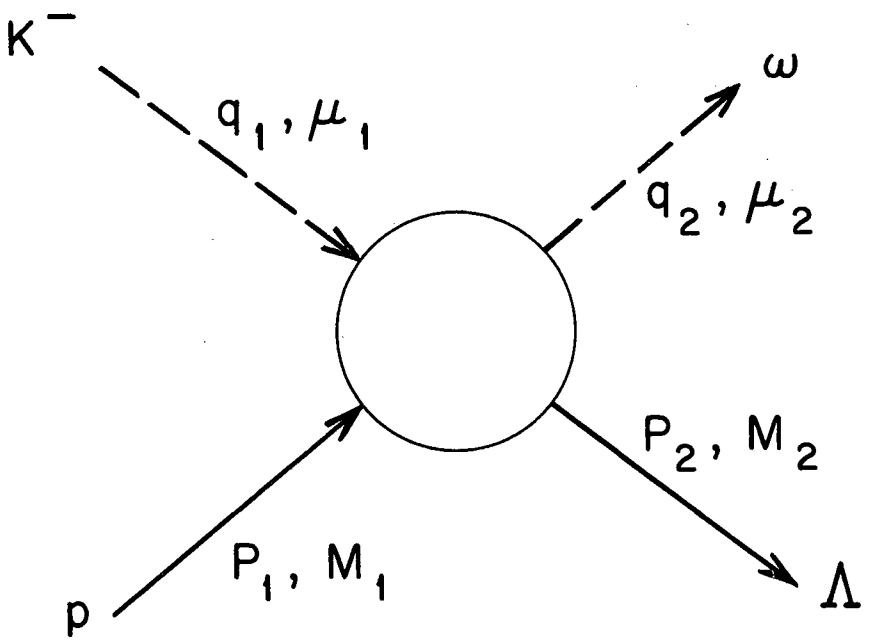

MUB-8405

Fig. 5

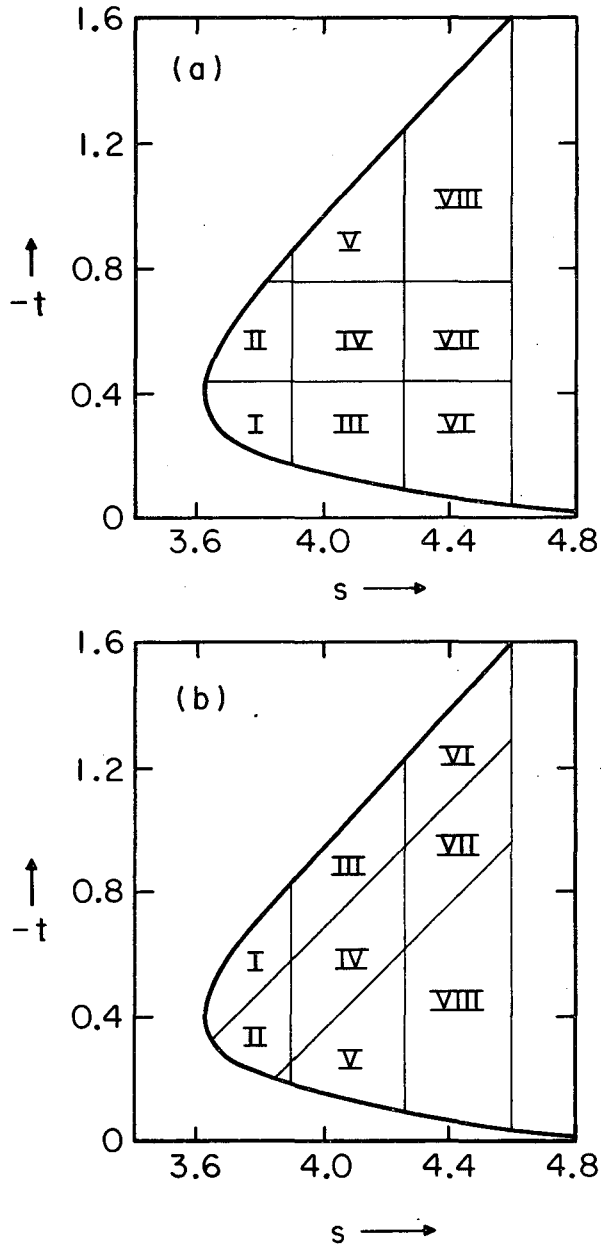

MUB-8407

Fig. 6

(ij) \ (kl)	−−	0−	+−	−+	0+	++
−−	$\lvert a_{--}\rvert^2$		$a^*_{--}a_{+-}$		$a^*_{--}a_{0+}$	
0−		$\lvert a_{0-}\rvert^2$		$a^*_{0-}a_{-+}$		$a^*_{0-}a_{++}$
+−	$a^*_{+-}a_{--}$		$\lvert a_{+-}\rvert^2$		$a^*_{+-}a_{0+}$	
−+		$a^*_{-+}a_{0-}$		$\lvert a_{-+}\rvert^2$		$a^*_{-+}a_{++}$
0+	$a^*_{0+}a_{--}$		$a^*_{0+}a_{+-}$		$\lvert a_{0+}\rvert^2$	
++		$a^*_{++}a_{0-}$		$a^*_{++}a_{-+}$		$\lvert a_{++}\rvert^2$

MUB-8408

Fig. 7

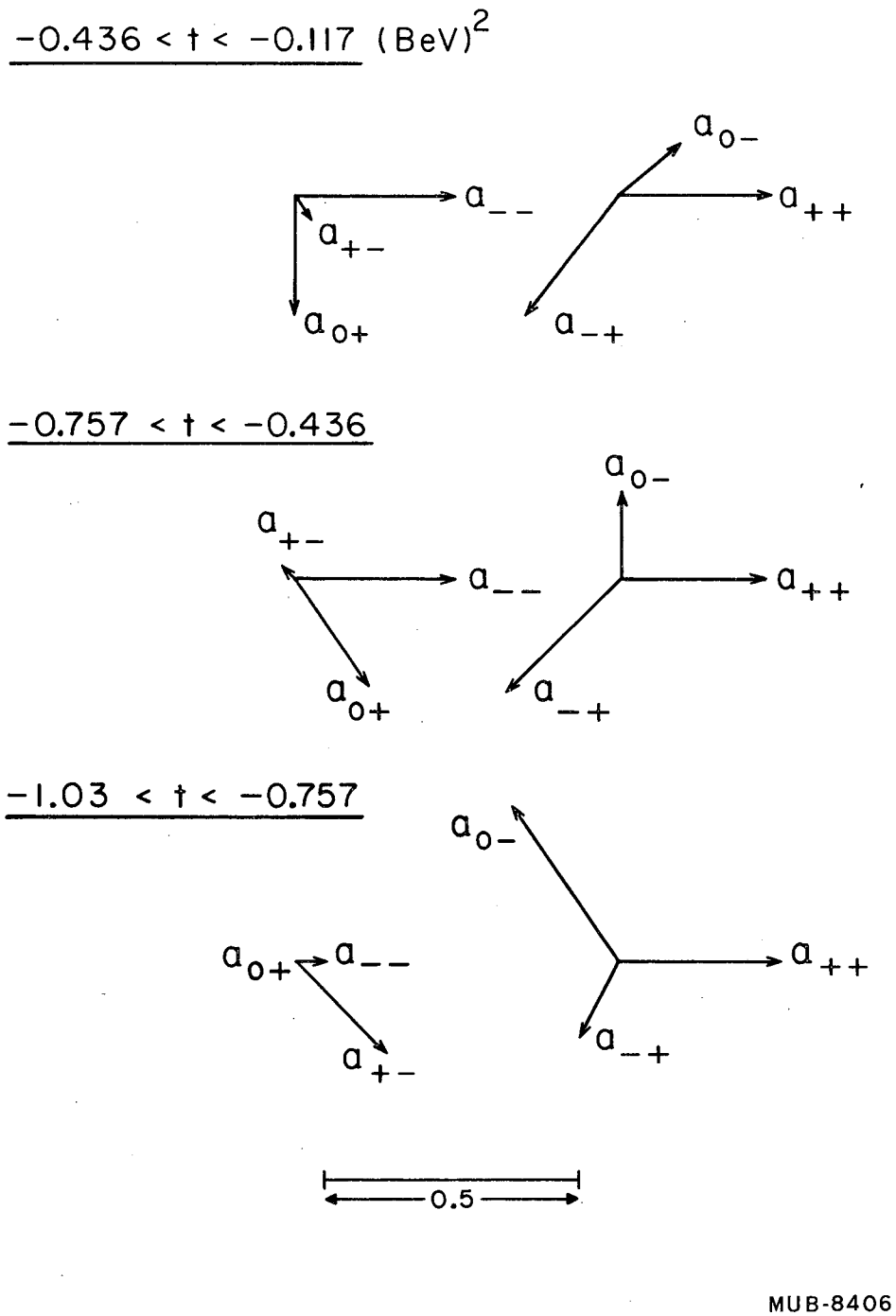
-0.436 < t < -0.117 (BeV)^2
a_{0-}
a_{--}
a_{++}
a_{+-}
a_{0+}
a_{-+}
-0.757 < t < -0.436
a_{0-}
a_{+-}
a_{--}
a_{++}
a_{0+}
a_{-+}
-1.03 < t < -0.757
a_{0-}
a_{0+}
a_{--}
a_{++}
a_{+-}
a_{-+}
0.5
MUB-8406

Fig. 8

This report was prepared as an account of Government sponsored work. Neither the United States, nor the Commission, nor any person acting on behalf of the Commission:

A. Makes any warranty or representation, expressed or implied, with respect to the accuracy, completeness, or usefulness of the information contained in this report, or that the use of any information, apparatus, method, or process disclosed in this report may not infringe privately owned rights; or

B. Assumes any liabilities with respect to the use of, or for damages resulting from the use of any information, apparatus, method, or process disclosed in this report.

As used in the above, "person acting on behalf of the Commission" includes any employee or contractor of the Commission, or employee of such contractor, to the extent that such employee or contractor of the Commission, or employee of such contractor prepares, disseminates, or provides access to, any information pursuant to his employment or contract with the Commission, or his employment with such contractor.